Published in final edited form as:
Development. 2008 June ; 135(12): 2065–2070. doi:10.1242/dev.022673.

Cell cycle progression is required for zebrafish somite morphogenesis but not segmentation clock function

Lixia Zhang, **Christina Kendrick**, **Dörthe Jülich**, and **Scott A. Holley**
Department of Molecular, Cellular and Developmental Biology, Yale University, New Haven, CT 06520

Summary

Cell division, differentiation and morphogenesis are coordinated during embryonic development and frequently in disarray in pathologies such as cancer. Here, we present a zebrafish mutant that ceases mitosis at the beginning of gastrulation, but undergoes axis elongation and develops blood, muscle and a beating heart. We identify the mutation as being in *early mitotic inhibitor 1* (*emi1*), a negative regulator of the Anaphase Promoting Complex, and utilize the mutant to examine the role of the cell cycle in somitogenesis. The mutant phenotype indicates that axis elongation during the segmentation period is substantially driven by cell migration. We find that the segmentation clock, which regulates somitogenesis, functions normally in the absence of cell cycle progression and observe that mitosis is a modest source of noise for the clock. Somite morphogenesis involves the epithelialization of the somite border cells around a core of mesenchyme. As in wild-type embryos, somite boundary cells are polarized along a Fibronectin matrix in *emi1*$^{-/-}$. The mutants also display evidence of segment polarity. However, in the absence of a normal cell cycle, somites appear to hyper-epithelialize as the internal mesenchymal cells exit the core of the somite after initial boundary formation. Thus, cell cycle progression is not required during the segmentation period for segmentation clock function but is necessary for normal segmental arrangement of epithelial borders and internal mesenchymal cells.

Keywords

somitogenesis; cell cycle; zebrafish; emi1; somite morphogenesis

Introduction

Somites are the segmented precursors to the axial skeleton and musculature created as the trunk and tail elongates. The periodic formation of somites is governed by the segmentation clock which creates oscillations in gene expression in the presomitic mesoderm (PSM) (Pourquié, 2003). In zebrafish, the segmentation clock requires Notch signaling while the amniote clocks also incorporate Wnt and Fgf signaling (Holley, 2007). It is debated whether the Notch, Wnt or Fgf pathways constitute core components of the clock or if they are a readout of a global clock that governs all of embryonic development (Aulehla et al., 2003; Dequeant et al., 2006; Niwa et al., 2007; Wahl et al., 2007). For instance, there are models linking the segmentation clock to the cell cycle oscillator (Collier et al., 2000; McInerney et al., 2004; Primmett et al., 1989; Primmett et al., 1988).

Somite morphogenesis occurs as the segment boundary cells undergo a mesenchymal to epithelial transition (MET) forming a ball of cells with an epithelial surface and a core of

Correspondence: scott.holley@yale.edu.

mesenchyme (Holley, 2007). Zebrafish somite morphogenesis requires the transcription factor *fused somites*/*tbx24* (*fss*), Eph/Ephrin signaling and *integrin α5*/*fibronectin* function (Barrios et al., 2003; Durbin et al., 1998; Durbin et al., 2000; Jülich et al., 2005a; Koshida et al., 2005; Nikaido et al., 2002; van Eeden et al., 1996). *fss* links the segmentation clock and somite morphogenesis (Holley et al., 2000). *fss* mutants fail to maintain the segmentation clock in the anterior PSM, lack segment polarity and *ephA4* expression, and exhibit a complete loss of MET in the paraxial (somitic) mesoderm (Durbin et al., 2000; Holley et al., 2000; Oates et al., 2005b; van Eeden et al., 1998). Exogenous expression of *ephA4* in genetic mosaics can induce boundaries in $fss^{-/-}$ embryos (Barrios et al., 2003). Similarly in mouse genetic mosaics, *ephA4* expression correlates with boundary formation (Nakajima et al., 2006). Integrin α5-GFP clusters along the basal side of nascent somite boundary cells, and *integrin α5* and its ligand *fibronectin* are required for the maintenance and full maturation of the boundary in zebrafish, mice and *Xenopus* (Georges-Labouesse et al., 1996; Goh et al., 1997; Jülich et al., 2005a; Koshida et al., 2005; Kragtorp and Miller, 2007; Yang et al., 1993). Double mutants between *integrin α 5* and the Notch pathway lead to a complete loss of MET in the paraxial mesoderm (Jülich et al., 2005a). Simultaneous loss of *ephrin B2a*, a ligand for *ephA4*, and *integrin α 5* leads to a synergistic defect in somite boundary morphogenesis (Koshida et al., 2005). Ena/Vasp and Fak, which function in Integrin signaling, are necessary for somite formation in *Xenopus* (Kragtorp and Miller, 2006). Chick somite morphogenesis is regulated by *snail2* and *cdc42* which promote mesenchymal cell morphology and *rac1* which fosters epithelial cell morphology (Dale et al., 2006; Nakaya et al., 2004).

Emi1 is a negative regulator of the Anaphase Promoting Complex (APC) and is required for entry into mitosis in *Xenopus* embryos (Reimann et al., 2001). APC, an E3 ubiquitin ligase, also functions in post-mitotic cells. In *Drosophila* and *C. elegans* neurons, APC localizes to the synapse and regulates turnover of glutamate receptors (Juo and Kaplan, 2004; van Roessel et al., 2004). In vertebrate neurons, inhibition of APC by RNA interference or over-expression of *emi1* increases axonal growth and overcomes much of the growth-inhibitory effects of myelin. In contrast to the synapse studies, virtually all of the APC is located in the nuclei of these neurons, and the axon growth phenotype appears to be due to stabilization of Id2 and SnoN (Lasorella et al., 2006; Stegmuller et al., 2006).

Here, we identify a zebrafish mutant for *emi1* which ceases mitosis at the beginning of gastrulation. Using this mutant, we find that normal cell cycle progression is not required for segmentation clock function, but rather that mitosis is a modest source of noise for the clock. Finally, we show that the cell cycle defect leads to hyper-epithelialization of the somites after initiation of morphological segmentation.

Materials and Methods

Zebrafish breeding, mapping and cloning

Breeding and meiotic mapping followed standard protocols (Geisler, 2002; Nüsslein-Volhard and Dahm, 2002). The coding sequence of *emi1* (Genbank: NM_001003869) was isolated via RT-PCR and cloned into pCS2+. This clone was used to generate sense mRNA using the Ambion SP6 mMessage Machine kit and anti-sense riboprobe using the Roche digoxygenin labeling mix. For allele sequencing, we used *emi1* template from two independently derived *tiy121* RT-PCRs. Wild-type embryos were injected with 0.5 mM *emi1* morpholino targeting the splice donor of the second intron (5′-tgattgtcgtttcacctcatcatct-3′).

Immunohistochemistry, in situ hybridization

Fibronectin, phalloidin and S58 staining (Jülich et al., 2005a) and fluorescent in situ hybridization with β-catenin immunohistochemistry (Jülich et al., 2005b) were performed as previously described. All in situ hybridizations were performed with digoxygenin-labeled riboprobes. *her1* and *deltaC* antisense probes were made from plasmid clones as previously described (Holley et al., 2000; Holley et al., 2002). The *tbx18*, *mesogenin*, *mesp-b*, and *ripply1* coding sequences were isolated via RT-PCR and subjected to an additional round of PCR in which a T7 promoter was added in the antisense orientation. Antisense riboprobes were then created using T7 RNA polymerase (NEB). Integrin α5-GFP (Jülich et al., 2005a) and YFP-Emi1 were visualized with rabbit anti-GFP (1:1000) (Invitrogen) and anti-rabbit Alexa488 (1:200) (Invitrogen). Goat anti-EphrinB2 (1:500) (R&D Systems) was paired with anti-goat Alexa647 (1:200) (Invitrogen). Rabbit anti-Phospho-Histone H3 antibody (1:1000) (Sigma) was used with goat-anti-rabbit-HRP (1:400) (Invitrogen) and Fluorescein TSA (Perkin Elmer).

We analyzed *her1* expression in *emi1* mutant and sibling embryos injected with translation-blocking morpholinos against either *deltaC* or *deltaD* (Holley et al., 2002). Three independent trials were performed with embryos derived from different parents and injected on different days. *deltaC* morpholino-injected and *deltaD* morpholino-injected embryos were fixed in 4% PFA at the ~2-somite and ~5 somite stages, respectively. Embryos were co-stained for *her1* expression with NBT/BCIP and fluorescently for PHH3. Absence of PHH3 staining was used to sort $emi1^{-/-}$ from sibling embryos. Classification of the expression patterns is described in the legend of Fig. 3.

Drug treatment and BrdU labeling

Embryos were incubated in 150 μM aphidicolin and 20 mM hydroxyurea (Sigma) in 4% DMSO starting at the germ ring/early shield stage and incubated until fixation (Harris and Hartenstein, 1991; Lyons et al., 2005). Drug treatment at this stage blocked mitosis by the late shield stage, mimicking the onset of the $emi1^{-/-}$ phenotype. To assay for DNA synthesis, 10 mM BrdU was injected into the yolk just after the shield, at the 1-somite and at the 8-somite stages. Embryos were fixed in 4% PFA at the 14–15 somite stage. BrdU incorporation was visualized using a mouse anti-BrdU antibody (1:200) (Sigma) and an Alexa-647-labeled goat anti-mouse antibody (1:200) (Invitrogen). Embryos injected at each stage showed BrdU incorporation indicating that endoreplication occurs continuously during late gastrulation and trunk segmentation in *emi1* mutants.

Results and Discussion

We identified a zebrafish mutant, *tiy121*, which exhibits a mitotic block (Fig. 1A-D). By the shield stage, mutant embryos cease all mitosis as visualized by immunostaining for phosphorylated Histone H3. Despite the mitotic arrest, mutant embryos undergo gastrulation and axis elongation (Fig. 1E,F). Measurement of the distance from the otic vesicle to the tip of the tail indicates that *tiy121* embryos (n=15) are on average 22% (s.d. ±3.2%) shorter than their wild-type siblings (n=17). After the mitotic block, mutant embryos continue endoreplication, as indicated by BrdU labeling (Fig. 1G,H). *tiy121* embryos ultimately develop a pericardial edema, extensive necrosis in the head and die 2–3 days post-fertilization. The relatively normal progression of early development in *tiy121* embryos parallels the finding that early *Xenopus* development is unperturbed by chemical inhibition of mitosis (Cooke, 1973; Harris and Hartenstein, 1991; Rollins and Andrews, 1991).

We mapped *tiy121* via meiotic recombination to chromosome 13 between the Simple Sequence Length Polymorphisms (SSLP) z24268 and z55656, near a zebrafish homologue

of *early mitotic inhibitor 1* (*emi1)* (Fig. 2A). Determination of the *emi1* coding sequence in the single mutant allele revealed a premature stop codon that truncates the protein prior to the F-box domain, likely creating an amorphic allele (Fig. 2B). Injection of a splice-blocking morpholino against *emi1* recapitulates the mitotic defect through gastrulation. However, the antisense inhibition declines by the tailbud stages, and mitosis is normal by the 5-somite stage (Fig. 2C). In morpholino injected embryos, Phosphorylated Histone H3 staining (PHH3) was absent (89%) or reduced (9%) at the shield stage (n=101), was reduced in 79% at the tailbud stage (n=39) and was indistinguishable from controls at the 5-somite stage (n=37). Injection of in vitro synthesized mRNA for *YFP-emi1* rescues the mitotic defect through gastrulation, but the rescue declines by the tailbud stage and is absent by the 18-somite stage (Fig. 2C). *YFP-emi1* mRNA (5 ng/μl) was injected into clutches from *tiy121*$^{-/+}$ parents. Normal PHH3 was seen in 99% (n=75) and 98% (n=141) of embryos at the shield and tailbud stage, respectively. By the 5-somite stage, 16% (n=110) showed reduced PHH3, and at the 18-somite stage, 27% (n=153) showed no PPH3. *tiy121* fails to complement *hi2648*, a hypomorphic, retroviral allele of *emi1* (Fig. 2D)(Amsterdam et al., 2004). Together, these data indicate that the *tiy121* phenotype is due to perturbation of *emi1*.

emi1 mRNA is maternally deposited (Fig. 2E) and later ubiquitously expressed in the blastula and gastrula (Fig. 2F). Emi1-YFP protein localizes to the nucleus but is diminished in cells undergoing mitosis (Fig. 2H-J). During segmentation, *emi1* is broadly expressed, including within the somites (Fig. 2G).

While *tiy121* embryos are short, the mutant phenotype indicates that cell proliferation is not absolutely required for trunk and tail extension. However, the mutants display irregularly sized and partially fused somites and myotomes (Fig. 3A-D; supplemental material). The segmentation clock creates oscillations in transcription that manifest as stripes of expression sweeping through the cells of the PSM in a wave-like fashion. We examined the expression of three oscillating genes *her1*, *her7* and *deltaC* at the 3-somite, 8-somite and 15-somite stage and found no appreciable defect in their expression in *emi1*$^{-/-}$ (Fig. 3E-J and data not shown). Note that at the 8 and 15-somite stage the tailbud of *emi1*$^{-/-}$ embryos is smaller than normal (compare Fig. 3F and G to I and J, respectively). This decrease is reflected in the reduction of the domain of *mesogenin* expression (supplementary material). While *emi1* mutants undergo mitosis at the beginning of gastrulation when oscillations are first seen (Riedel-Kruse et al., 2007), our data indicate that continued oscillation of the segmentation clock is not dependent upon the cell cycle.

In contrast to models that link the cell cycle to the segmentation clock, it has been postulated that mitosis is actually a source of noise for the clock (Horikawa et al., 2006). To test this hypothesis, we examined the effect of inhibiting mitosis in embryos lacking either of the Notch ligands *deltaC* or *deltaD*. The *deltaC* and *deltaD* mutants form the first 3–5 and 7–9 somites, respectively, as the oscillating pattern of gene expression gradually breaks down leading to the segmentation defect (Fig. 3K-N; supplemental material) (Holley et al., 2000; Jiang et al., 2000; Jülich et al., 2005b; Oates et al., 2005a; van Eeden et al., 1996; van Eeden et al., 1998). This breakdown may be accelerated due to noise. Thus, if mitosis is a source of noise in the segmentation program, one would predict that the breakdown would decelerate in the absence of cell division. We assayed the expression of *her1* mRNA in *deltaD* or *deltaC* morpholino-injected embryos that were either wild-type or mutant for *emi1* (Fig. 3N; supplemental material). The difference between the mutants and siblings was not immediately apparent. However, upon careful categorization of the expression patterns, we found a subtle improvement in the integrity of the *her1* stripes in embryos lacking *emi1* compared to sibling embryos. For each trial, the more organized stripe patterns are biased towards the injected *emi1* mutants, and the two more disorganized expression categories are

biased towards the injected siblings. In summary, these results are consistent with mitosis being a modest source of noise in the segmentation clock.

Further examination of the segmentation defect in *emi1*$^{-/-}$ embryos revealed profound abnormalities in somite morphology. While *emi1*$^{-/-}$ somites initially contain internal mesenchymal cells, these cells leave the core of the somite and, at least some, integrate into the epithelial somite boundary (Fig. 4A,B,D,E). We have observed other cells migrating to the lateral surface of the paraxial mesoderm. The somite boundary cells then appear to elongate and meet in the middle of each segment creating somites consisting solely of two rows of boundary cells (Fig. 4B,E,G,I). These hyper-epithelialized somites, having no internal mesenchyme and abnormally elongated epithelial border cells, often fuse to create irregularly sized segments. The nuclei of the boundary cells show a basal localization, as does Integrin α5-GFP clustering (Fig. 4A,B). Fibronectin matrix is also assembled along the somite boundaries (Fig. 4F,G). This maintenance of border cell polarity distinguishes the *emi1*$^{-/-}$ phenotype from that of the *integrin* α5 and *fibronectin1a* mutants (Jülich et al., 2005a; Koshida et al., 2005). Ephrin B2 is localized on the cortex of the somite cells with slightly higher levels in the posterior somite cells, and this pattern appears largely intact in the *emi1*$^{-/-}$ mutants (Fig. 4H,I; supplemental material). Expression of *mesp-b*, *ripply1* and *tbx18*, *myoD* and *deltaC* is clearly segmental though there is some aberrant expression of *deltaC* in the mutant embryos (Fig. 4J-M; supplementary material). The segment polarity alterations observed in *emi1* mutants are slight in comparison to those defects seen in *fss* and the Notch pathway mutants and seem unlikely to be the cause of the morphological phenotype.

The morphological analysis suggests that the polarity of the somite boundary cells is maintained. The somite phenotype also does not seem to follow from a defect in anterior-posterior patterning of the somites. Rather, it appears that the somites in *emi1*$^{-/-}$ mutant embryos are hyper-epithelialized. The hyper-epithelialization could be due to elevated APC activity, which may affect the stability of proteins involved in regulating cell morphology independently of the cell cycle (Juo and Kaplan, 2004; Konishi et al., 2004; Lasorella et al., 2006; Stegmuller et al., 2006; van Roessel et al., 2004). To test this hypothesis, we blocked mitosis using a combination of hydroxyurea and aphidicolin (Harris and Hartenstein, 1991; Lyons et al., 2005). Addition of the compounds at the germ ring/early shield stage blocked all mitosis by the late shield stage and resulted in embryos lacking internal mesenchymal cells in their somites, strongly phenocopying *emi1*$^{-/-}$ (Fig. 4C; supplemental material). These data suggest that the segmentation defect in *emi1*$^{-/-}$ mutant embryos is primarily due to the lack of normal cell cycle progression and not to a cell cycle independent function of *emi1* or APC. Note that in both mutant and drug-treated embryos, the cells and nuclei are larger than in wild-type (Fig. 4). The increase in cell size, along with the decrease in cell number, may also be causally linked to the somite morphogenesis defect.

The mitotic defect in *emi1*$^{-/-}$ embryos arises after the midblastula transition (MBT). MBT initiates during the 10th cell cycle (3 hpf) when divisions become asynchronous and zygotic transcription commences (Kane, 1999; Kane and Kimmel, 1993). During cycles 11 and 12, the blastula forms three domains, the extra-embryonic yolk syncytial layer and enveloping layer, and the deep cells that give rise to the embryo proper (Kane, 1999). At 5.5 hpf, gastrulation starts as most of the deep cells are in cell cycle 14 (Kane, 1999; Kane et al., 1992). *emi1*$^{-/-}$ embryos cease cell division around this time. In wild-type embryos, the cell cycle lengthens during this period, with the 13th, 14th, 15th and 16th cycles averaging 54, 78, 151 and 240 minutes, respectively. During segmentation, most cells are in either cell cycle 16 or 17 (Kane, 1999). The mild elongation defect in *emi1*$^{-/-}$ is likely due to the fact that mitosis is normally not a great contributor to axial growth during the segmentation period. This conclusion was also reached by examining the elongation of clonal strings of cells in

the CNS: the exponential lengthening of the string suggested that it was largely due to cell intercalation not cell division (Kimmel et al., 1994). The relatively normal differentiation in *emi1*$^{-/-}$ embryos can be explained by the fact that many cells undergo a terminal differentiation during cell cycle 15, 8–10 hpf, and a major wave of differentiation occurs during cycle 16 (Kane, 1999; Kimmel et al., 1994; Kimmel and Warga, 1987). Thus, for many cell lineages, the mitotic defect in *emi1* embryos does not dramatically reduce the number of cell cycles that these cells would normally undergo.

The cell cycle could in principle serve as a clock to regulate developmental timing (Johnson and Day, 2000). Experiments in ascidians have suggested that the timing of myogenesis may depend upon the number of cycles of DNA synthesis that a myogenic progenitor experiences (Satoh, 1987). However, previous cell labeling experiments indicate that zebrafish myofiber differentiation is not regulated by such a cell cycle counting mechanism (Kimmel and Warga, 1987). Similarly, expression of differentiation markers in the *C. elegans* gut occurs independently of cell cycle counting (Edgar and McGhee, 1988). The segmentation clock has been suggested to be linked to the cell cycle oscillator. Reiterated segmentation defects are seen in chick embryos after treatment with cell-cycle inhibitors, and the periodicity of this defect is equal to the cell cycle length at that stage of development (Primmett et al., 1989). Similar periodic defects were seen after a single heat shock (Primmett et al., 1988). More recently, this cell cycle model has been formalized mathematically (Collier et al., 2000; McInerney et al., 2004). In the zebrafish, a single heat shock can produce reiterated segmentation defects, but the periodicity of the defect does not correlate with the length of the cell cycle during segmentation (Roy et al., 1999). Additionally, there is no organized pattern of cell proliferation in the zebrafish tailbud (Kanki and Ho, 1997). Our analysis of the *emi1* mutant indicates that cell cycle progression is not required for zebrafish segmentation clock function. Conversely, our data are consistent with the hypothesis that mitosis is a modest source of noise for the segmentation clock (Horikawa et al., 2006).

Supplementary Material

Refer to Web version on PubMed Central for supplementary material.

Acknowledgments

We thank Hiroyuki Takeda and members of the lab for comments on the manuscript. The *tiy121* mutant was isolated in the Tübingen 2000 Screen, and we acknowledge all of participants of the consortium: F. Van Bebber, E. Busch-Nentwich, R. Dahm, O. Frank, H.-G. Fronhöfer, H. Geiger, D. Gilmour, S. Holley, J. Hooge, D. Jülich, H. Knaut, F. Maderspacher, H.-M. Maischein, C. Neumann, C. Nüsslein-Volhard, H. Roehl, U. Schönberger, C. Seiler, S. Sidi, M. Sonawane, A. Wehner, P. Erker, H. Habeck, U. Hagner, C. E. Hennen Kaps, A. Kirchner, T. Koblizek, U. Langheinrich, C. Loeschke, C. Metzger, R. Nordin, J. Odenthal, M. Pezzuti, K. Schlombs, J. de Santana-Stamm, T. Trowe, G. Vacun, B. Walderich, A. Walker & C. Weiler. We thank Nancy Hopkins for the *hi2648* allele. We thank Joseph Wolenski for assistance with the confocal microscopy. This work was supported by the March of Dimes Foundation, research grant number 1-FY07-424, and the NICHD, R01 HD045738.

References

Amsterdam A, Nissen RM, Sun Z, Swindell EC, Farrington S, Hopkins N. Identification of 315 genes essential for early zebrafish development. Proc Natl Acad Sci U S A 2004;101:12792–7. [PubMed: 15256591]

Aulehla A, Wehrle C, Brand-Saberi B, Kemler R, Gossler A, Kanzler B, Herrmann BG. Wnt3a Plays a Major Role in the Segmentation Clock Controling Somitogenesis. Dev Cell 2003;4:395–406. [PubMed: 12636920]

Barrios A, Poole RJ, Durbin L, Brennan C, Holder N, Wilson SW. Eph/Ephrin signaling regulates the mesenchymal-to-epithelial transition of the paraxial mesoderm during somite morphogenesis. Curr Biol 2003;13:1571–82. [PubMed: 13678588]

Collier JR, McInerney D, Schnell S, Maini PK, Gavaghan DJ, Houston P, Stern CD. A cell cycle model for somitogenesis: mathematical formulation and numerical simulation. J Theor Biol 2000;207:305–16. [PubMed: 11082301]

Cooke J. Morphogenesis and regulation in spite of continued mitotic inhibition in Xenopus embryos. Nature 1973;242:55–7. [PubMed: 4694293]

Dale JK, Malapert P, Chal J, Vilhais-Neto G, Maroto M, Johnson T, Jayasinghe S, Trainor P, Herrmann B, Pourquie O. Oscillations of the snail genes in the presomitic mesoderm coordinate segmental patterning and morphogenesis in vertebrate somitogenesis. Dev Cell 2006;10:355–66. [PubMed: 16516838]

Dequeant ML, Glynn E, Gaudenz K, Wahl M, Chen J, Mushegian A, Pourquie O. A complex oscillating network of signaling genes underlies the mouse segmentation clock. Science 2006;314:1595–8. [PubMed: 17095659]

Durbin L, Brennan C, Shiomi K, Cooke J, Barrios A, Shanmugalingam S, Guthrie B, Lindberg R, Holder N. Eph signaling is required for segmentation and differentiation of the somites. Genes Dev 1998;12:3096–109. [PubMed: 9765210]

Durbin L, Sordino P, Barrios A, Gering M, Thisse C, Thisse B, Brennan C, Green A, Wilson S, Holder N. Anteriorposterior patterning is required within segments for somite boundary formation in developing zebrafish. Development 2000;127:1703–1713. [PubMed: 10725246]

Edgar LG, McGhee JD. DNA synthesis and the control of embryonic gene expression in C. elegans. Cell 1988;53:589–99. [PubMed: 3131016]

Geisler, R. Mapping and Cloning. In: Nusslein-Volhard, C.; Dahm, R., editors. Zebrafish. Oxford, UK: Oxford University Press; 2002. p. 175-212.

Georges-Labouesse EN, George EL, Rayburn H, Hynes RO. Mesodermal development in mouse embryos mutant for fibronectin. Dev Dyn 1996;207:145–56. [PubMed: 8906418]

Goh KL, Yang JT, Hynes RO. Mesodermal defects and cranial neural crest apoptosis in alpha5 integrin-null embryos. Development 1997;124:4309–19. [PubMed: 9334279]

Harris WA, Hartenstein V. Neuronal determination without cell division in Xenopus embryos. Neuron 1991;6:499–515. [PubMed: 1901716]

Holley SA. The genetics and embryology of zebrafish metamerism. Dev Dyn 2007;236:1422–49. [PubMed: 17486630]

Holley SA, Geisler R, Nüsslein-Volhard C. Control of *her1* expression during zebrafish somitogenesis by a *Delta*-dependent oscillator and an independent wave-front activity. Genes & Dev 2000;14:1678–1690. [PubMed: 10887161]

Holley SA, Jülich D, Rauch GJ, Geisler R, Nüsslein-Volhard C. her1 and the notch pathway function within the oscillator mechanism that regulates zebrafish somitogenesis. Development 2002;129:1175–83. [PubMed: 11874913]

Horikawa K, Ishimatsu K, Yoshimoto E, Kondo S, Takeda H. Noise-resistant and synchronized oscillation of the segmentation clock. Nature 2006;441:719–23. [PubMed: 16760970]

Jiang YJ, Aerne BL, Smithers L, Haddon C, Ish-Horowicz D, Lewis J. Notch signaling and the synchronization of the somite segmentation clock. Nature 2000;408:475–479. [PubMed: 11100729]

Johnson MH, Day ML. Egg timers: how is developmental time measured in the early vertebrate embryo? Bioessays 2000;22:57–63. [PubMed: 10649291]

Jülich D, Geisler R, Consortium TS, Holley SA. Integrinα5 and Delta/Notch Signalling have Complementary Spatiotemporal Requirements during Zebrafish Somitogenesis. Dev Cell 2005a: 575–86.

Jülich D, Lim CH, Round J, Nicolaije C, Davies A, Schroeder J, Geisler R, Consortium TS, Lewis J, Jiang YJ, et al. beamter/deltaC and the role of Notch ligands in the zebrafish somite segmentation, hindbrain neurogenesis and hypochord differentiation. Dev Biol 2005b;286:391–404.

Juo P, Kaplan JM. The anaphase-promoting complex regulates the abundance of GLR-1 glutamate receptors in the ventral nerve cord of C. elegans. Curr Biol 2004;14:2057–62. [PubMed: 15556870]

Kane DA. Cell cycles and development in the embryonic zebrafish. Methods Cell Biol 1999;59:11–26. [PubMed: 9891352]

Kane DA, Kimmel CB. The zebrafish midblastula transition. Development 1993;119:447–56. [PubMed: 8287796]

Kane DA, Warga RM, Kimmel CB. Mitotic domains in the early embryo of the zebrafish. Nature 1992;360:735–7. [PubMed: 1465143]

Kanki JP, Ho RK. The development of the posterior body in zebrafish. Development 1997;124:881–893. [PubMed: 9043069]

Kimmel CB, Warga RM, Kane DA. Cell cycles and clonal strings during formation of the zebrafish central nervous system. Development 1994;120:265–276. [PubMed: 8149908]

Kimmel CB, Warga RW. Cell lineages generating axial muscle in the zebrafish embryo. Nature 1987;327:234–237. [PubMed: 3574488]

Konishi Y, Stegmuller J, Matsuda T, Bonni S, Bonni A. Cdh1-APC controls axonal growth and patterning in the mammalian brain. Science 2004;303:1026–30. [PubMed: 14716021]

Koshida S, Kishimoto Y, Ustumi H, Shimizu T, Furutani-Seiki M, Kondoh H, Takada S. Integrinalpha5-Dependent Fibronectin Accumulation for Maintenance of Somite Boundaries in Zebrafish Embryos. Dev Cell 2005;8:587–598. [PubMed: 15809040]

Kragtorp KA, Miller JR. Regulation of somitogenesis by Ena/VASP proteins and FAK during Xenopus development. Development 2006;133:685–95. [PubMed: 16421193]

Kragtorp KA, Miller JR. Integrin alpha5 is required for somite rotation and boundary formation in Xenopus. Dev Dyn 2007;236:2713–20. [PubMed: 17685483]

Lasorella A, Stegmuller J, Guardavaccaro D, Liu G, Carro MS, Rothschild G, de la Torre-Ubieta L, Pagano M, Bonni A, Iavarone A. Degradation of Id2 by the anaphase-promoting complex couples cell cycle exit and axonal growth. Nature 2006;442:471–4. [PubMed: 16810178]

Lyons DA, Pogoda HM, Voas MG, Woods IG, Diamond B, Nix R, Arana N, Jacobs J, Talbot WS. erbb3 and erbb2 are essential for schwann cell migration and myelination in zebrafish. Curr Biol 2005;15:513–24. [PubMed: 15797019]

McInerney D, Schnell S, Baker RE, Maini PK. A mathematical formulation for the cell-cycle model in somitogenesis: analysis, parameter constraints and numerical solutions. Math Med Biol 2004;21:85–113. [PubMed: 15228101]

Nakajima Y, Morimoto M, Takahashi Y, Koseki H, Saga Y. Identification of Epha4 enhancer required for segmental expression and the regulation by Mesp2. Development 2006;133:2517–25. [PubMed: 16728472]

Nakaya Y, Kuroda S, Katagiri YT, Kaibuchi K, Takahashi Y. Mesenchymal-epithelial transition during somitic segmentation is regulated by differential roles of Cdc42 and Rac1. Dev Cell 2004;7:425–38. [PubMed: 15363416]

Nikaido M, Kawakami A, Sawada A, Furutani-Seiki M, Takeda H, Araki K. Tbx24, encoding a T-box protein, is mutated in the zebrafish somite-segmentation mutant fused somites. Nat Genet 2002;31:195–9. [PubMed: 12021786]

Niwa Y, Masamizu Y, Liu T, Nakayama R, Deng CX, Kageyama R. The initiation and propagation of Hes7 oscillation are cooperatively regulated by Fgf and notch signaling in the somite segmentation clock. Dev Cell 2007;13:298–304. [PubMed: 17681139]

Nüsslein-Volhard, C.; Dahm, R. Zebrafish. In: Hames, BD., editor. Practical Approach. Oxford, UK: Oxford University Press; 2002. p. 303

Oates AC, Mueller C, Ho RK. Cooperative function of deltaC and her7 in anterior segment formation. Dev Biol 2005a;280:133–49. [PubMed: 15766754]

Oates AC, Rohde LA, Ho RK. Generation of segment polarity in the paraxial mesoderm of the zebrafish through a T-box-dependent inductive event. Dev Biol 2005b;283:204–14. [PubMed: 15921674]

Pourquié O. The segmentation clock: converting embryonic time into spatial pattern. Science 2003;301:328–30. [PubMed: 12869750]

Primmett DR, Norris WE, Carlson GJ, Keynes RJ, Stern CD. Periodic segmental anomalies induced by heat shock in the chick embryo are associated with the cell cycle. Development 1989;105:119–130. [PubMed: 2806112]

Primmett DR, Stern CD, Keynes RJ. Heat shock causes repeated segmental anomalies in the chick embryo. Development 1988;104:331–9. [PubMed: 3254821]

Reimann JD, Freed E, Hsu JY, Kramer ER, Peters JM, Jackson PK. Emi1 is a mitotic regulator that interacts with Cdc20 and inhibits the anaphase promoting complex. Cell 2001;105:645–55. [PubMed: 11389834]

Riedel-Kruse IH, Muller C, Oates AC. Synchrony dynamics during initiation, failure, and rescue of the segmentation clock. Science 2007;317:1911–5. [PubMed: 17702912]

Rollins MB, Andrews MT. Morphogenesis and regulated gene activity are independent of DNA replication in Xenopus embryos. Development 1991;112:559–69. [PubMed: 1794324]

Roy MN, Prince VE, Ho RK. Heat shock produces periodic somitic disturbances in the zebrafish embryo. Mech Dev 1999;85:27–34. [PubMed: 10415344]

Satoh N. Towards a Molecular Understanding of Differentiation Mechanisms in Ascidian Embryos. Bioessays 1987;7:51–56.

Stegmuller J, Konishi Y, Huynh MA, Yuan Z, Dibacco S, Bonni A. Cell-intrinsic regulation of axonal morphogenesis by the Cdh1-APC target SnoN. Neuron 2006;50:389–400. [PubMed: 16675394]

van Eeden FJM, Granato M, Schach U, Brand M, Furutani-Seiki M, Haffter P, Hammerschmidt M, Heisenberg CP, Jiang YJ, Kane DA, et al. Mutations affecting somite formation and patterning in the zebrafish *Danio rerio*. Development 1996;123:153–164. [PubMed: 9007237]

van Eeden FJM, Holley SA, Haffter P, Nüsslein-Volhard C. Zebrafish segmentation and pair-rule patterning. Dev Genet 1998;23:65–76. [PubMed: 9706695]

van Roessel P, Elliott DA, Robinson IM, Prokop A, Brand AH. Independent regulation of synaptic size and activity by the anaphase-promoting complex. Cell 2004;119:707–18. [PubMed: 15550251]

Wahl MB, Deng C, Lewandoski M, Pourquie O. FGF signaling acts upstream of the NOTCH and WNT signaling pathways to control segmentation clock oscillations in mouse somitogenesis. Development 2007;134:4033–41. [PubMed: 17965051]

Yang JT, Rayburn H, Hynes RO. Embryonic mesodermal defects in alpha 5 integrin-deficient mice. Development 1993;119:1093–105. [PubMed: 7508365]

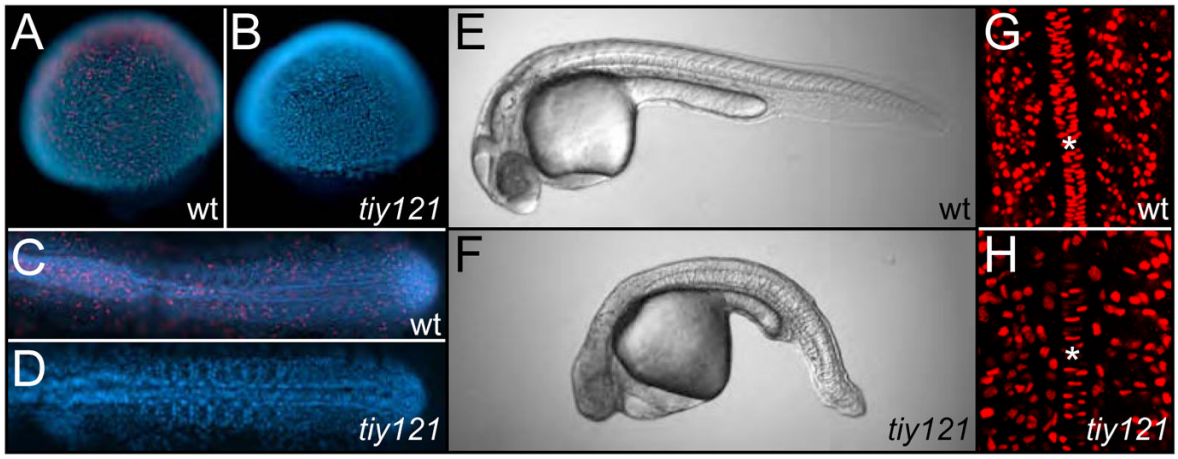

Fig. 1. *tiy121* mutants have a cell cycle defect

(A) Phosphorylated histone H3 staining (PHH3) (red) marks mitotic cells in wild-type embryos at the shield (A) and 10-somite stage (C). No mitotic nuclei are seen in *tiy121* embryos at the shield (B) or 12-somite stage (D). Nuclei are stained with DAPI (blue). Wild-type (E) and *tiy121*$^{-/-}$ (F) embryos at 30 hours post fertilization (hpf). BrdU labeling (red) in the trunks of wild-type (G) and *tiy121*$^{-/-}$ (H) at the 14-somite stage. Asterisks label the notochord. BrdU was injected into the yolk at the 8-somite stage. In C-F, Anterior is left. In G and H, anterior is up.

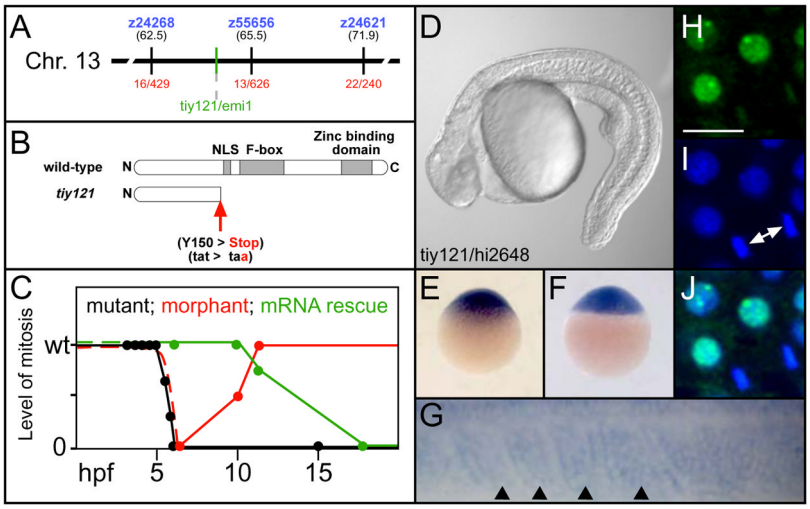

Fig. 2. *tiy121* is an *emi1* mutant

(A) The chromosomal location of *tiy121/emi1*. (B) *tiy121* is a premature stop codon in *emi1*. NLS, nuclear localization signal. (C) A graph of the level of mitosis in *tiy121*, *emi1* morphants, and *tiy121* embryos rescued by injection of *emi1* mRNA. Morphants and mRNA injected embryos develop normally prior to the shield stage, thus we infer that the initial level of mitosis is normal without examining PHH3 (dashed lines). The level of mitosis is either wild-type (wt), reduced to some degree, or mitosis is absent. Hours post fertilization, hpf. (D) *tiy121* and *hi2648*, an insertional allele of *emi1*, do not complement. Expression of *emi1* mRNA at (E) the one cell stage, (F) sphere stage and (G) the most recently formed somites (arrowheads) and anterior PSM of a 12-somite stage embryo. Anterior is left in G. (H) YFP-Emi1. (I) DAPI stained nuclei. (J) overlay of H and I. Arrows indicate a cell completing mitosis. Scale bar is 20 μm.

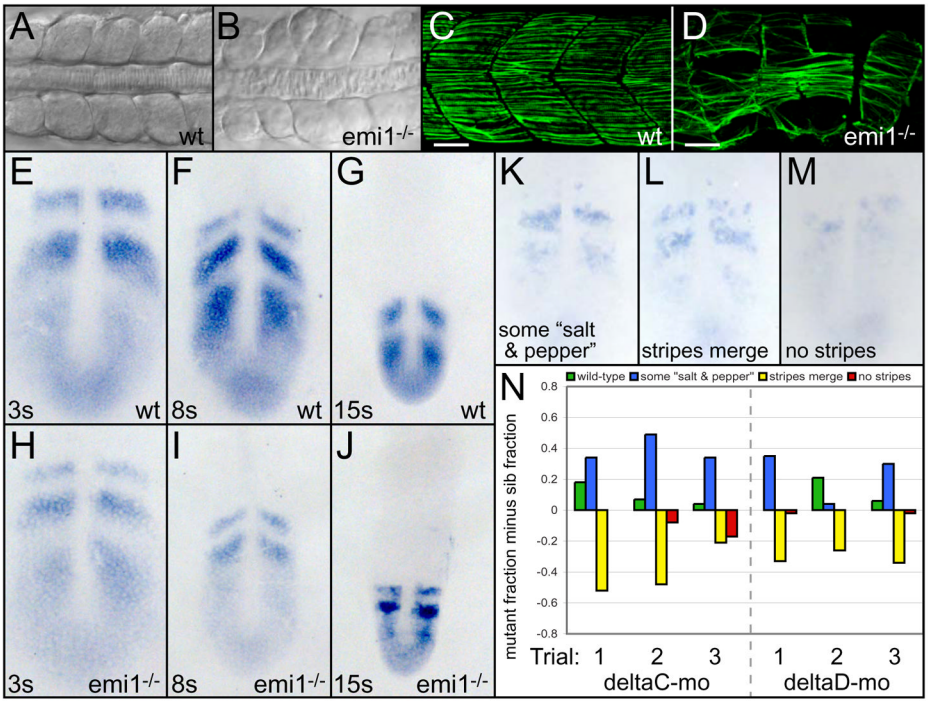

Fig. 3. Cell cycle progression is necessary for somitogenesis but not segmentation clock function

Dorsal views of anterior trunk somites in wild-type (A) and *emi1*$^{-/-}$ (B) embryos at the 15-somite stage. Posterior trunk myotomes of wild-type (C) and *emi1*$^{-/-}$ (D) embryos at 36 hpf. Slow muscle fibers are labeled with S58 antibodies (green). Scale bars are 30 μm. *her1* expression at the (E,H) 3-somite, (F,I) 8-somite and (G,J) 15-somite stages in (E-G) wild-type and (H-J) *emi1*$^{-/-}$ embryos. (K-N) *her1* stripe integrity was examined in *emi1*$^{-/-}$ and sibling embryos injected with morpholinos against either *deltaC* or *deltaD. her1* expression was rated according to four categories representing increasing loss of organized expression: wild-type, (K) stripes with some salt and pepper expression, (L) stripes begin to merge, and (M) no stripes. (N) Distributions of gene expression patterns are displayed for three independent trials (x-axis). Within each gene expression category, the fraction of sibling embryos is subtracted from the fraction of mutant embryos. For example, the wild-type category in the first *deltaC* morpholino trial included 0.20 fraction of the mutant embryos (20%) and 0.02 fraction of the sibling embryos (2%), giving a graphed value of 0.18. In *deltaC* morpholino trials, the number of mutants and siblings assayed (mutant/sib) are: 39/74, 27/79 and 16/57. For *deltaD* morpholino trials, the corresponding numbers are: 60/50, 28/74 and 49/90. Given the subjective nature of the expression classification, a second assayer performed an independent blind classification of the same embryos (supplemental material). While the profiles of the distributions differ, the distinction between *emi1* and sibling embryos was consistent. In A-D, anterior is left. In E-M, anterior is up.

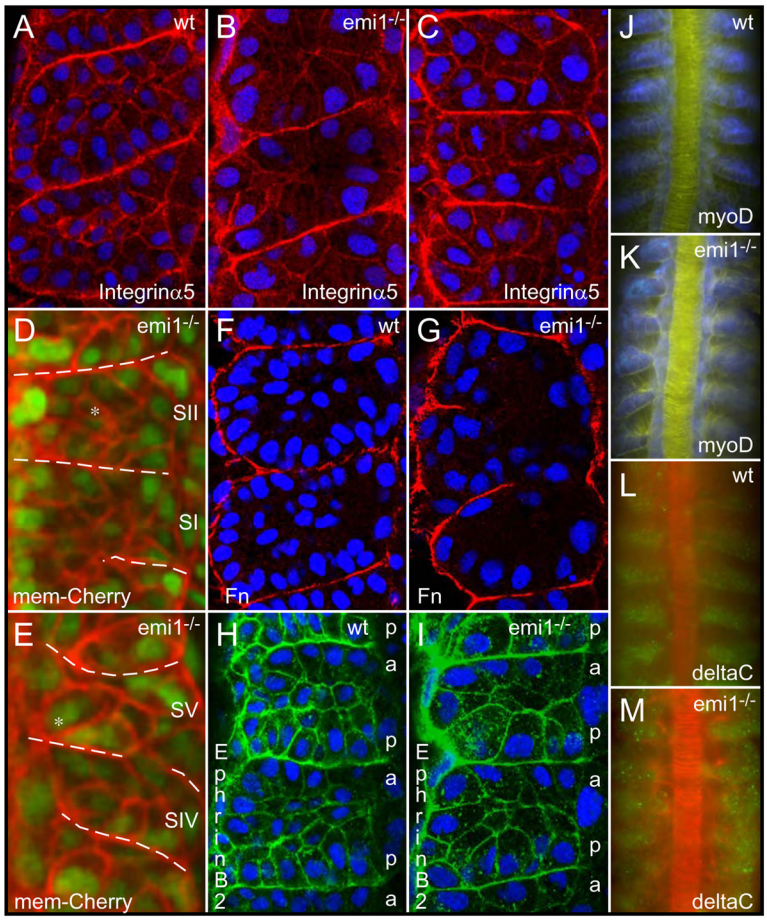

Fig. 4. Cell cycle progression is required for normal somite morphogenesis

Integrin α5-GFP (red) labels the cell cortex and clusters along somite borders in (A) wild-type (wt), (B) *emi1*$^{-/-}$ and (C) aphidocolin-hydroxyurea treated embryos. Embryos are at the 12-somite stage. Somites 2–4, 3–5 and 3–5 are shown, respectively. (D, E) show the same somites at the beginning (SI and SII) and end (SIV and SV, respectively) of a timelapse. The somite borders are indicated with the dashed lines. Somites initially have internal mesenchymal cells, but after 3 somite cycles have passed, the internal mesenchymal cells (* in D) have moved to the surface of the somite (* in E). Membrane localized cherry, mem-cherry (red). Fibronectin (Fn) matrix (red) forms along the borders in (F) wt and (G) *emi1*$^{-/-}$. Embryos are at the 12-somite stage. Somites 6–7 and 3–5 are pictured. Ephrin B2 expression (green) shows a graded, segmental distribution in (H) wt and (I) *emi1*$^{-/-}$. The lateral membranes of the posterior (p) somite border cells show higher levels of Ephrin B2 than the lateral membranes of anterior (a) border cells. Embryos are at the 12-somite stage. Shown are somites 5–6 and 4–5. Segmental expression of *myoD* (blue) in (J) wt, somites 3–8, and (K) *emi1*$^{-/-}$, somites 4–9, in 10-somite stage embryos. Expression of *deltaC* (green) in (L) wt, somites 4–9, is aberrant but segmental in (M) *emi1*$^{-/-}$, somites 4–9, in 10-somite stage embryos. Nuclei are labeled with DAPI (blue) in A-C and F-I. In D and E, nuclei are labeled with nuclear-GFP (green). β-catenin labels the cell cortex in J,K (yellow) and L,M (red). In all panels, anterior is up.